European Journal of Medicinal Chemistry 64 (2013) 629–637

Contents lists available at SciVerse ScienceDirect

European Journal of Medicinal Chemistry

journal homepage: http://www.elsevier.com/locate/ejmech

Original article

Synthesis and pharmacological properties of a new hydrophilic and orally bioavailable 5-HT$_4$ antagonist

Bjarne Brudeli [a,d], Lise Román Moltzau [b,c], Cam H.T. Nguyen [b,c], Kjetil Wessel Andressen [b,c], Nils Olav Nilsen [a], Finn Olav Levy [b,c], Jo Klaveness [a,d,*]

[a] Drug Discovery Laboratory AS, Oslo Innovation Center, N-0349 Oslo, Norway
[b] Department of Pharmacology, Faculty of Medicine, University of Oslo and Oslo University Hospital, P.O. Box 1057, Blindern, N-0316 Oslo, Norway
[c] K.G. Jebsen Cardiac Research Centre and Center for Heart Failure Research, Faculty of Medicine, University of Oslo, N-0316 Oslo, Norway
[d] Department of Medicinal Chemistry, School of Pharmacy, University of Oslo, N-0316 Oslo, Norway

ARTICLE INFO

Article history:
Received 17 October 2012
Received in revised form
22 March 2013
Accepted 27 March 2013
Available online 9 April 2013

Keywords:
Bioavailability
hERG
5-HT$_4$ antagonist
Hydrophilic
Pharmacokinetic
Prodrug

ABSTRACT

5-HT$_4$ receptor antagonists have been suggested to have clinical potential in treatment of atrial fibrillation, diarrhea-prone irritable bowel syndrome and urinary incontinence. Recently, the use of 5-HT$_4$ antagonists has been suggested to have a therapeutic benefit in heart failure. Affinity for the hERG potassium ion channel and increased risk for prolonged QT intervals and arrhythmias has been observed for several 5-HT$_4$ ligands. Serotonin may also have beneficial effects in the central nervous system (CNS) through stimulation of the 5-HT$_4$ receptor, and reduced distribution of 5-HT$_4$ antagonists to the CNS may therefore be an advantage. Replacing the amide and *N*-butyl side chain of the 5-HT$_4$ receptor antagonist SB207266 with an ester and a benzyl dimethyl acetic acid group led to compound **9**; a hydrophilic 5-HT$_4$ antagonist with excellent receptor binding and low affinity for the hERG potassium ion channel. To increase oral bioavailability of carboxylic acid **9**, two different prodrug approaches were applied. The *tert*-butyl prodrug **11** did not improve bioavailability, and LC-MS analysis revealed unmetabolized prodrug in the systemic circulation. The medoxomil ester prodrug **10** showed complete conversion and sufficient bioavailability of **9** to advance into further preclinical testing for treatment of heart failure.

1. Introduction

Serotonin (5-hydroxytryptamine; 5-HT) is a monoaminergic neurotransmitter in the central and peripheral nervous system. Today, 14 different human serotonin receptors are known, divided into 7 distinct families (5-HT$_{1-7}$) [1]. Pharmaceuticals acting on serotonin receptors play important roles in several pathological conditions. The first line treatment of migraine is triptans, a class of selective serotonin agonists that affect the 5-HT$_{1B}$ and 5-HT$_{1D}$ receptors in cranial artery smooth muscle [2]. Nausea and emesis after chemotherapy are treated with e.g. ondansetron and tropisetron, selective serotonin antagonists that affect the 5-HT$_3$ receptor in the chemoreceptor trigger zone and the gastro-intestinal system.

Serotonin causes increased rate and force of contraction through 5-HT$_4$ receptors in human atria [3]. Recent investigations have revealed that the human cardiac ventricles show increased response to serotonin through 5-HT$_4$ receptors in infarcted and failing hearts [4]. Further, increased expression of the 5-HT$_4$ receptor may indicate a role of the serotonergic system in this condition. Recently, blocking of the 5-HT$_4$ receptor has been investigated in both experimental animals and humans, and the use of 5-HT$_4$ receptor antagonists may be a new therapeutic intervention in treatment of congestive heart failure [5,6].

Irritable bowel syndrome (IBS) is a gastrointestinal disorder characterized by abdominal pain, bloating and altered bowel habits. An increased understanding of the role of serotonin in regulation of GI motility, secretion and visceral sensitivity has led to the development of 5-HT receptor modulators for treatment of IBS [7]. Both the 5-HT$_3$ receptor antagonists alosetron and cilansetron and the 5-HT$_4$ agonists cisapride and tegaserod have been developed for treatment of diarrhea- and constipation-predominant forms of IBS, respectively. However, serious side effects have led to market withdrawal or suspension of these agents. Post market findings revealed that cisapride binds to the human *ether-à-go-go* related gene (hERG) potassium channel, an ion channel important for the cardiac action potential. High affinity for this channel can give rise to prolonged QT interval and cause fatal torsades des pointes arrhythmia [8].

* Corresponding author. School of Pharmacy, University of Oslo, P.O. Box 1068, Blindern, N-0316 Oslo, Norway. Tel.: +47 22855043; fax: +47 22857975.
E-mail address: jo.klaveness@farmasi.uio.no (J. Klaveness).

0223-5234/$ – see front matter © 2013 Elsevier Masson SAS. All rights reserved.
http://dx.doi.org/10.1016/j.ejmech.2013.03.060

Increased focus on hERG has revealed strategies to avoid drug binding to this ion channel, and the incorporation of negatively-charged functional groups seems to be a feasible way to overcome hERG potassium channel-related side effects [9]. This strategy can also be used to avoid distribution of peripheral-acting drugs to the central nervous system, and it has been successfully introduced to second-generation antihistamine H_1-receptor antagonists. All second-generation anti-allergic drugs contain a carboxylic acid group, or they are metabolized to active metabolites with a carboxylic acid group [10]. Terfenadine, a H_1-receptor antagonist with a *tert*-butyl group, is extensively metabolized to the corresponding dimethyl acetic acid metabolite fexofenadine as outlined in Fig. 1. Fexofenadine, in contrast to terfenadine, does not bind to the hERG channel and has limited CNS distribution because of the negatively charged carboxylate group. However, reports of prolonged QT intervals and arrhythmias due to incomplete metabolic conversion of terfenadine to fexofenadine have led to market withdrawal of terfenadine. Only the carboxylic acid metabolite fexofenadine is used today in anti-allergic treatment. It has also been shown that the carboxylic acid group is important for antihistamine drugs to act as substrates for P-glycoproteins, and second generation antihistamines are actively transported out of the central nervous system [11].

We have previously reported the synthesis and pharmacological effects of some novel hydrophilic 5-HT_4 receptor antagonists [12]. Since 5-HT_4 agonists might have beneficial effects in the central nervous system, reduced distribution of 5-HT_4 antagonists to the CNS may be an advantage. Reducing the risk of cardiotoxic side effects like prolonged QT interval may be achieved by increasing the hydrophilicity of new therapeutic 5-HT_4 ligands, for example by incorporating a carboxylic acid moiety [9]. We have therefore prepared a new hydrophilic 5-HT_4 receptor antagonist **9** that has structural similarities with the second-generation H_1-antagonist fexofenadine as shown in Fig. 2. The dimethyl acetic acid antagonist **9** shows promising 5-HT_4 receptor binding and low affinity for the hERG potassium channel. The log $D_{Oct7.4}$ value also indicates low distribution to the central nervous system, a clinical benefit since reduced CNS side effects may be expected.

However, the hydrophilic carboxylic acid **9** showed limited oral bioavailability in a rat model. To increase oral bioavailability of the new antagonist, two different prodrug approaches were applied. First the corresponding *tert*-butyl prodrug **11** was synthesized and evaluated with respect to oral bioavailability. The *tert*-butyl derivative **11** did not improve bioavailability, and plasma analysis revealed incomplete metabolism to carboxylic acid **9**. Therefore, the corresponding medoxomil ester prodrug **10** was prepared. The medoxomil ester **10** showed both complete conversion to carboxylic acid **9** and satisfactory oral bioavailability and pharmacokinetics.

2. Chemistry

The hydrophilic carboxylic acid **9**, a derivative of the 5-HT_4 antagonist SB207266, and the corresponding prodrugs **10** and **11** are shown in Fig. 2.

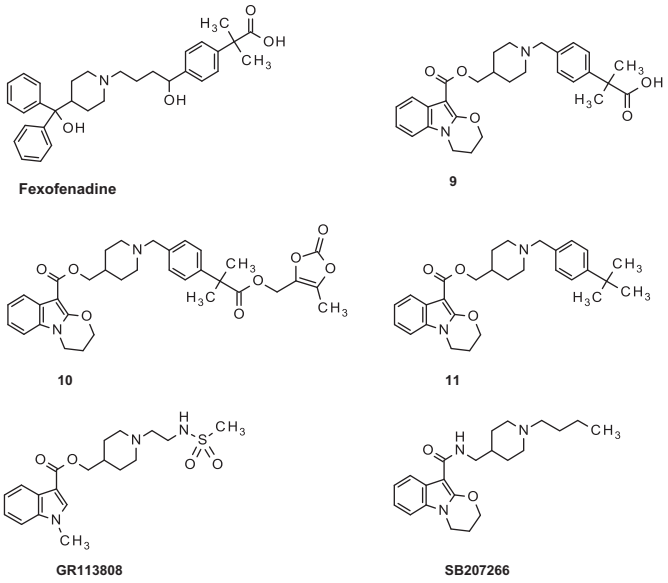

Fig. 2. Structures of fexofenadine, GR113808, SB207266 and the synthesized derivatives **9**–**11**.

The synthesis of benzyl-protected piperidine derivative **3** and the corresponding de-protected amine **4** is shown in Scheme 1. The synthesis of indole ester **1** and piperidine methanol derivative **2** has been described elsewhere [13,14]. The benzyl protected intermediate **3** was prepared by adding n-BuLi to a cooled solution of piperidine methanol derivative **2** in THF, followed by indole ester **1** and stirring to room temperature. Crystallization from EtOAc gave intermediate **3** in 89% yield. Hydrogenation of benzyl intermediate **3** using Pd/C at 5 bar in a mixture of glacial acetic acid and methanol at room temperature gave the de-protected amine **4** in 81% yield.

The synthesis of the bromide intermediate **7** is shown in Scheme 2. Alkylation of 2-(4-methylphenyl)propanoic acid with MeI in DMF in the presence of $NaHCO_3$ at room temperature gave the methyl ester **5** in 95% yield. Addition of **5** to a cooled suspension of NaH in n-hexane, followed by MeI and stirring at room temperature gave intermediate **6** in 49% yield. Addition of N-bromosuccinimide to a solution of **6** in dichloromethane followed by benzoyl peroxide and heating the mixture to reflux gave the bromo derivative **7** in 61% yield after filtration of the reaction mixture through a pad of silica.

The synthesis of carboxylic acid **9** and the corresponding prodrug ester **10** is shown in Scheme 3. Addition of bromo derivative **7** to a solution of amine **4** in acetone in the presence of K_2CO_3 and heating the mixture to reflux gave the methyl ester **8** in 45% yield after purification with column chromatography. Hydrolysis of methyl ester **8** with sodium hydroxide in a mixture of aqueous MeOH under reflux gave carboxylic acid **9** in 45% yield. Alkylation of carboxylic acid **9** with 4-chloromethyl-5-methyl-1,3-dioxol-2-one in DMA in the

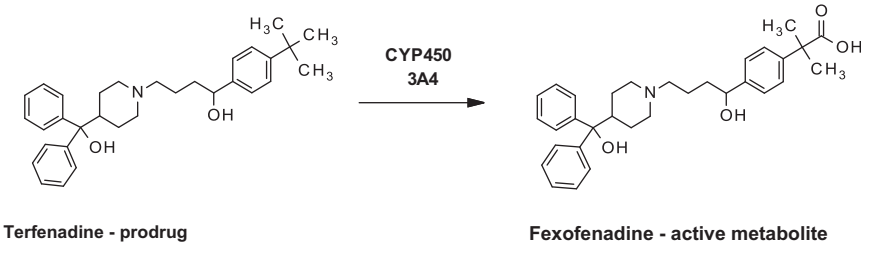

Fig. 1. First-pass metabolism of the second generation H_1 receptor antagonist terfenadine to the active metabolite fexofenadine.

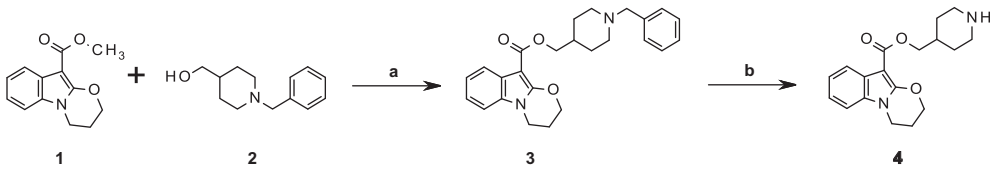

Scheme 1. Reagents and conditions: a) n-BuLi, THF, 0 °C ➔ room temperature; b) H_2, Pd–C 20%, CH_3CO_2H/MeOH, room temperature.

presence of K_2CO_3 under reflux gave the prodrug ester **10** in 50% yield after purification with column chromatography.

The synthesis of the *tert*-butyl derivative **11** is shown in Scheme 4. Alkylation of piperidine amine **4** with 4-(*tert*-butyl)-1-benzyl bromide in acetone in the presence of K_2CO_3 under reflux gave the *tert*-butyl derivative **11** in 59% yield after purification with column chromatography.

3. Pharmacology

Binding affinities and 5-HT_4 antagonist properties were determined for GR113808, SB207266 and compound **9** and **11** by competitive binding and concentration-dependent inhibition of 5-HT-stimulated adenylyl cyclase (AC) activity in membranes from HEK293 cells stably expressing the human 5-$HT_{4(b)}$ receptor. pK_i-values and pK_b-values from competition of [^{3}H] GR113808 binding and from antagonism of 5-HT_4-stimulated adenylyl cyclase activity, respectively, for GR113808, SB207266 and compounds **9** and **11** are summarized in Table 1.

Reduction of hERG tail current of compound **9** was quantified with the patch-clamp technique in HEK293 cells stably transfected with hERG ion channel cDNA. Peak hERG tail current amplitude was measured prior to and following exposure to compound **9** at different concentrations. Terfenadine, a known inhibitor of the I_{Kr} current, was used as a positive control.

Oral bioavailability and pharmacokinetic properties of compounds **9**, **10** and **11** were determined in male Sprague-Dawley rats. The concentration of compound **9** in plasma was measured by liquid chromatography-mass spectrometry (LC-MS) after oral dosing of **9**, **10** and **11**. To calculate the oral bioavailability, compound **9** was also administered by intravenous (i.v.) dosing. The pharmacokinetic calculations for tentative bioavailability (F, %), maximum plasma concentration (C_{max}, ng/ml), clearance (CL, ml/min/kg), half-life ($T_{1/2,}$ min) and time to reach maximum plasma concentration (T_{max}, min) are shown in Table 2.

The in vitro stability and metabolic profile of compound **9** was determined in human liver microsomes. Metabolic degradation of **9** and identification of metabolites was analyzed by LC-MS.

4. Results and discussion

The 5-HT_4 receptor binding site is extensively described in literature [15]. The pharmacophore antagonist model features an aromatic ring, a coplanar carbonyl group and an alkaline nitrogen substituted with a bulky group [16]. Carboxylic acid **9** fulfills these

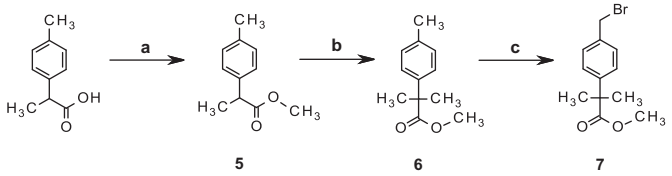

Scheme 2. Reagents and conditions: a) MeI, $NaHCO_3$, DMF, room temperature; b) MeI, NaH, n-hexane, room temperature; c) NBS, BPO, CH_2Cl_2, reflux.

criteria, and the binding affinity and adenylyl cyclase data were measured to pK_i 9.9 ± 0.2 and pK_b 8.6 ± 0.1, respectively.

New drug candidates are commonly tested across a panel of side-effect targets. One of these is the affinity for the hERG potassium channel. High affinity for this ion channel may indicate a risk of prolonged QT intervals and serious cardiac arrhythmias [17]. Several in vitro tests are available to screen out possible hERG channel blockers, but the whole cell patch-clamp technique is regarded the most reliable method to measure interaction with the potassium channel [18]. Compound **9** was tested by the patch-clamp technique and the peak hERG tail amplitude was reduced by 55.8 ± 5.9% prior to and following exposure of a 100 μM solution. The corresponding IC_{50} value was estimated to 69.0 μM ($n = 3$) after fitting the data points with a sigmoidal function. A 50 nM solution of terfenadine, a known inhibitor of the I_{Kr} current, inhibited 69.4 ± 3.1% in the same assay. Based on binding and AC assays, the therapeutic concentration of a 5-HT_4 antagonist with intended pharmacodynamic action in the human ventricle is expected to be in the low-nanomolar range. Therefore, it is unlikely that compound **9** will block the hERG potassium channel and provoke cardiac arrhythmias in a clinical situation. This finding is also consistent with previous results obtained with 5-HT_4 ligands containing carboxylic acid groups [12].

Screening of absorption, distribution, metabolism and excretion (ADME) properties is important in the early discovery and lead-optimization phases for a new drug. Orally active drugs are absorbed from the intestine, transported by the portal vein to the liver before reaching the systemic circulation. After the drug enters the systemic circulation it is distributed from the blood and into different organs and tissues. Several variables like molecular weight, active transport mechanisms and plasma protein binding are important for the ADME properties of the drugs. Lipophilicity of the drug compound is also regarded as an important factor. Several methods are used to determine lipophilicity, but the distribution coefficient is the most commonly used. Assuming passive diffusion, the logarithmic distribution coefficient is often used to obtain a rough estimate of a drugs distribution and permeation properties. Hydrophilic drugs with negative values of log $D_{Oct7.4}$ are assumed to stay in hydrophilic compartments, have less systemic toxicity and are excreted from the body by renal clearance. More hydrophobic drugs with positive values are more likely to be metabolized by first pass metabolism in the liver, penetrate membranes and accumulate in organs and tissues such as the central nervous system [19–23].

The logarithmic partition coefficient between 1-octanol and phosphate buffer pH 7.4 was determined using the shake-flask method to −1.2 ± 0.1 for the carboxylic acid **9**. The relatively small log $D_{Oct7.4}$ value is caused by deprotonation of the carboxylic acid to the more water soluble carboxylate anion. The lead compound SB207266 and prodrugs **10** and **11** are significantly less water soluble with log $D_{Oct7.4}$ values ranging from 2.2 ± 0.1 to 2.4 ± 0.1. Even though more extensive animal studies are needed to determine the distribution and permeation patterns of these compounds, the log $D_{Oct7.4}$ value indicates that the carboxylic acid **9** will tend to have reduced CNS distribution compared to SB207266. This may be an advantage since the intended therapeutic use for a new hydrophilic 5-HT_4 antagonist will be in the cardiovascular

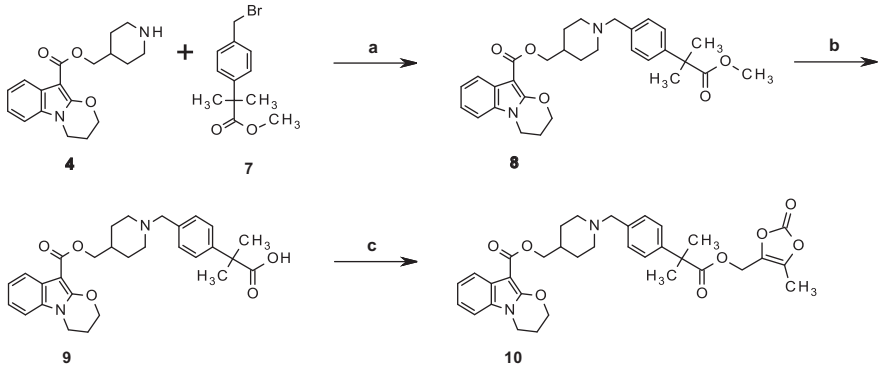

Scheme 3. Reagents and conditions: a) K_2CO_3, acetone, reflux; b) NaOH, MeOH/H_2O, reflux; c) 4-chloromethyl-5-methyl-1,3-dioxol-2-one, K_2CO_3, DMA, reflux.

system of heart failure patients [5,6]. Hydrophilic 5-HT_4 antagonists may also have therapeutic benefits in other peripheral organs and tissues like the intestine and urinary system. Further, it has been shown that stimulation of 5-HT_4 receptors seems to play a vital role in cognitive function through the release of acetylcholine and amyloid precursor protein (APP) peptides [24,25]. Reduced distribution into the CNS may therefore be important to avoid unwanted side effects of a new 5-HT_4 receptor antagonist.

The pharmacokinetic parameters for compounds **9**, **10** and **11** are summarized in Table 2, and the corresponding plasma concentrations versus time curves are shown in Fig. 3. To evaluate the potential for new compounds to be orally active, a threshold area under the curve (AUC) value of 500 h*ng/ml after a single 10 mg/kg oral dose to rat has been proposed [26]. The obtained total oral AUC for compound **9** was 285 ± 10 h*ng/ml, and the calculated tentative oral bioavailability 3%.

A strategy to increase oral bioavailability for H_1-receptor antagonists is shown in Fig. 1. The *tert*-butyl prodrug terfenadine is oxidized in the liver to the dimethyl acetic acid fexofenadine. Therefore, to increase oral bioavailability of dimethyl acetic acid **9**, we decided to use the same strategy and the *tert*-butyl prodrug **11** was prepared. However, the obtained total AUC for carboxylic acid **9** after administration of prodrug **11** was only 127 ± 16 h*ng/ml, corresponding to a bioavailability of 1%.

Unlike the second generation H_1-receptor antagonist terfenadine, where the *tert*-butyl group is completely metabolized to the active dimethyl acetic acid metabolite fexofenadine, LC-MS analysis revealed considerably amounts of unmetabolized **11** in plasma. The AUC for **11** was 533 ± 65 h*ng/ml, corresponding to a bioavailability of 6%. Despite incomplete metabolic oxidation to carboxylic acid **9**, the low AUC value may indicate extensive liver degradation of **11**. It was concluded that the *tert*-butyl prodrug strategy, as applied for fexofenadine, was not applicable for the dimethyl acetic acid **9**.

The maximum plasma concentration of compound **9** was reached at 12 ± 3 and 80 ± 20 min after administration of compound **9** and **11**, respectively. The difference in T_{max} is not unexpected since compound **11** needs to be metabolized to the acid **9** before reaching the circulatory system. A contributing factor can also be the possible lower solubility of compound **11** in the rat intestine. The calculated elimination half-life for compound **9** after oral administration of **9** and **11** was 364 ± 113 and 1190 ± 339 min, respectively. The difference in elimination half-life also indicates that the absorption and conversion phase has an impact on the elimination of the carboxylic acid **9**. The plasma clearance for compound **9** is 17 ± 1 ml/min/kg and is in the intermediate range when compared to typical rat liver blood flow of 55 ml/min [27]. The theoretical maximal bioavailability (F_{max}) for compound **9** would therefore be:

$$F_{max} = (1 - \text{Clearance/Liver blood flow}) \times 100\ \% = (1 - 17.2\ \text{ml/min/55 ml/min}) \times 100\ \% = 68\ \%.$$

The reasons for lower bioavailability can be degradation in the gastrointestinal tract, poor permeability or extensive first-pass metabolism. The relatively low T_{max} eliminates that poor permeability would be the only reason for low bioavailability. More likely the observed pharmacokinetics could be explained by extensive first-pass metabolism. This has also been seen in previous studies with 5-HT_4 ligands with aromatic ester functionalities [28].

To determine if the limited oral bioavailability was due to extensive liver degradation, the in vitro stability of compound **9** in human liver microsomes was evaluated. The concentration of carboxylic acid **9** in the in vitro assay was followed by LC-MS, indicating negligible metabolic degradation.

The microsome assay was also screened for potential degradation products, and two metabolites were detected. The abundance of these metabolites was low, less than 0.1% in the 60 min incubation sample. LC-time-of-flight (TOF)-MS analysis identified the degradation products as mono- and di-hydroxylated metabolites, where the hydroxyl groups were situated in the indole-oxazino ring system. Similar hydroxylated metabolites have previously been reported for the lead compound SB207266 [14].

Since the in vitro disappearance is slow and the predicted liver metabolic clearance negligible, it can be assumed that the limited bioavailability in rat is not solely caused by extensive first-pass metabolism. The observed difference between in vitro and in vivo

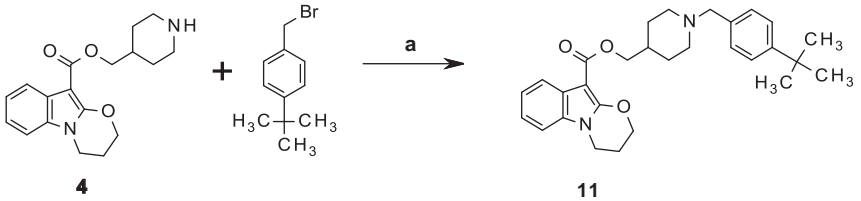

Scheme 4. Reagents and conditions: a) K_2CO_3, acetone, reflux.

Table 1
Logarithmic distribution coefficient (log $D_{Oct7.4}$) from an octanol/buffer distribution, pK_i-values from competition of [^{3}H] GR113808 binding, pK_b-values from antagonism of 5-HT-stimulated adenylyl cyclase activity of GR113808, SB207266 and compounds **9**–**11**.

Compound	log $D_{Oct7.4}$ ± SEM[a]	pK_i ± SEM[b]	pK_b ± SEM[c]	Molecular formula
GR113808	ND	10.4 ± 0.2	8.7 ± 0.1	$C_{19}H_{27}N_3O_4S$
SB207266	2.2 ± 0.1	10.0 ± 0.1	9.1 ± 0.1	$C_{22}H_{31}N_2O_2$
9	−1.2 ± 0.1	9.9 ± 0.2	8.6 ± 0.1	$C_{29}H_{34}N_2O_5$
10	2.2 ± 0.1	ND	ND	$C_{34}H_{38}N_2O_8 \times HCl$
11	2.4 ± 0.1	ND	ND	$C_{29}H_{36}N_2O_3 \times HCl$

[a] $n = 3$.
[b] $n = 3$–8.
[c] $n = 4$–7.

clearance is probably due to species differences in metabolism, active excretion to urine/bile or some non-liver degradation pathway. Despite the low T_{max} value of dimethyl acetic acid **9**, reduced absorption from the gastrointestinal tract may be a plausible explanation of limited oral bioavailability.

Preparation of ester prodrugs to increase passive diffusion through the intestinal wall is a well-known strategy [29]. The medoxomil ester prodrug is used to increase oral bioavailability of olmesartan, an angiontensin II receptor antagonist used in treatment of high blood pressure [30]. The olmesartan medoxomil ester prodrug has an oral bioavailability of 25% in humans. The medoxomil ester is completely metabolized to olmesartan carboxylic acid in the intestinal wall and liver, and no other component than the active olmesartan metabolite has been detected in plasma after oral administration [31,32]. To increase oral bioavailability of **9** and to minimize systemic concentrations of prodrug, the medoxomil ester prodrug **10** was synthesized and evaluated in the same animal model.

The pharmacokinetic parameters for compound **10** are summarized in Table 2, and the corresponding plasma concentration versus time curve for compound **9** is shown in Fig. 3. The total oral AUC for carboxylic acid **9** was 1206 h*ng/ml after administration of prodrug **10**, well above the threshold value of 500 h*ng/ml. The tentative oral bioavailability increased from 3% for the dimethyl acetic acid **9** to 16% for the corresponding medoxomil ester prodrug **10**. The stability of **9** in liver microsomes suggests that the oral bioavailability may be higher in other animal species or humans. The maximum peak plasma concentration and elimination half-life was found to be 30 and 72 min respectively. The medoxomil prodrug **10** was not detected in any of the harvested plasma samples.

5. Conclusion

We have synthesized a new hydrophilic 5-HT$_4$ receptor antagonist **9** with a benzyl dimethyl acetic acid group. The new antagonist shows excellent receptor binding and antagonism of 5-HT$_4$-mediated adenylyl cyclase activity. The hydrophilic derivative has minor affinity for the hERG ion channel and with a partition coefficient of −1.2, reduced CNS accumulations may be expected. The limited oral bioavailability can be overcome by administration of the medoxomil ester prodrug **10**. Further studies with the hydrophilic 5-HT$_4$ antagonist **9** as a new therapeutic opportunity in treatment of heart failure are planned in the future.

Table 2
Pharmacokinetic (PK) data for carboxylic acid **9** after administration of compound **9**–**11** in rats.

Compound	AUC (hr*ng/ml)	C_{max} (ng/ml)	T_{max} (min)	$T_{1/2}$ (min)	CL (ml/min/kg)	%F
9[a]	285 ± 10	130 ± 40	12 ± 3	364 ± 113	17 ± 1	3
10[b]	1206	817	30	72	NA	16
11[c]	127 ± 16	13 ± 4	80 ± 20	1190 ± 339	18 ± 3	1
11[d]	533 ± 65	33 ± 5	340 ± 140	1610 ± 483	20 ± 5	6

[a] PK of **9** after p.o. administration of **9** ($n = 3$).
[b] PK of **9** after p.o. administration of **10** ($n = 2$).
[c] PK of **9** after p.o. administration of **11** ($n = 3$).
[d] PK of **11** after p.o. administration of **11** ($n = 3$).

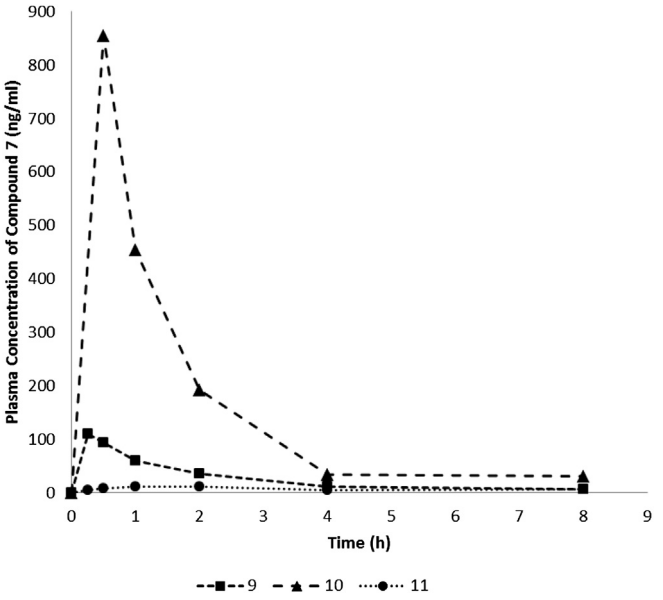

Fig. 3. Mean plasma concentration–time profiles of compound **9** after oral administration of compound **9** (■; $n = 3$), **10** (▲; $n = 2$) and **11** (●; $n = 3$) at a dose of 10 mg/kg in rats.

6. Experimental section

6.1. Chemistry

^{1}H NMR spectra were recorded on a Bruker Spectrospin Avance spectrometer at 300 MHz for ^{1}H and 75 MHz for ^{13}C. Chemical shifts are reported in parts per million relative to internal tetramethylsilane, residual $CHCl_3$ (δ_H = 7.26 ppm, δ_C = 77.0 ppm) or CHD_2SOCD_3 (δ_H = 2.50 ppm, δ_C = 39.43 ppm). Coupling constants (*J*) are reported in hertz (Hz). The following abbreviations are used to describe peak patterns when appropriate: s (singlet), d (doublet), t (triplet), q (quartet), m (multiplet) and br (broad). Analytical thin-layer chromatography (TLC) was run on Merck silica gel plates (Kieselgel 60 F-254) with UV-light or iodine detection. For flash chromatography, Fluka silica gel type 60 (size 200–400 mesh) was used. All solvents and reagents were of analytical or reagent grade and were obtained from commercial sources.

(1-Benzyl-4-piperidinyl)methanol **1** and methyl 3,4-dihydro-2*H*-[1,3]oxazino[3,2-*a*]-indole-10-carboxylate **2** were synthesized according to literature procedures [13,14].

6.1.1. Preparation of (1-benzyl-4-piperidinyl)methyl 3,4-dihydro-2H-[1,3]oxazino[3,2-a]indole-10-carboxylate (3)

1.6 M n-BuLi in THF (25.3 ml, 40.5 mmol) was added dropwise to a solution of piperidine methanol **2** (8.35 g, 40.5 mmol) in THF (50 ml) at 0 °C under argon atmosphere and stirred for 5 min. Methyl ester **1** (6.26 g, 27.1 mmol) was then added and the reaction mixture stirred at room temperature for 12 h. The reaction mixture was carefully hydrolyzed with water (30 ml) and extracted with CH_2Cl_2 (100 ml). The organic layer was washed with water (3 × 30 ml), dried over anhydrous Na_2SO_4, filtered and

concentrated in vacuo to leave an oil. The residue was treated with EtOAc and the precipitate filtered off to leave the title compound **3** as a white solid (9.70 g, 89%). ^{1}H NMR ($CDCl_3$): δ 7.96–7.93 (m, 1H), 7.31–7.10 (m, 8H), 4.50 (t, J = 5.2 Hz, 2H), 4.17 (d, J = 6.2 Hz, 2H), 4.06 (t, J = 6.2 Hz, 2H), 3.49 (s, 2H), 2.93–2.87 (m, 2H), 2.32–2.27 (m, 2H), 2.05–1.78 (m, 5 H), 1.45–1.39 (m, 2H). MS (ES): 405.2 $[M + H]^+$.

*6.1.2. Preparation of 4-piperidinylmethyl 3,4-dihydro-2H-[1,3] oxazino[3,2-a]indole-10-carboxylate (**4**)*

A solution of benzyl amine **3** (9.70 g, 24.0 mmol) in a mixture of glacial acetic acid (15 ml) and MeOH (80 ml) was hydrogenated over 20% Pd/C (1.0 g) and 5 bar at room temperature for 48 h. The reaction mixture was filtered and the filtrate diluted with H_20 (30 ml). The filtrate was made alkaline with K_2CO_3 to pH 11 and the aqueous mixture extracted with CH_2Cl_2 (3 × 50 ml). The organic layers were combined and dried over anhydrous Na_2SO_4, filtered and evaporated in vacuo to leave the title compound **4** as a white solid (6.12 g, 81%). ^{1}H NMR (DMSO-d_6): δ 7.83–7.79 (m, 1H), 7.28–7.26 (m, 1H), 7.14–7.07 (m, 2H), 4.51 (t, J = 4.7 Hz, 2H), 4.17–4.04 (m, 4H), 3.26–3.20 (m, 2H), 2.86–2.80 (m, 2H), 2.27–2.22 (m, 2H), 1.95–1.81 (m, 3H), 1.60–1.50 (m, 2H). MS (ES): 315.2 $[M + H]^+$.

*6.1.3. Preparation of methyl 2-(4-methylphenyl)propanoate (**5**)*

MeI (8.64 g, 76.1 mmol) was added dropwise to a mixture of 2-(4-methylphenyl)propanoic acid (5.00 g, 30.5 mmol) and $NaHCO_3$ (6.39 g, 76.1 mmol) in DMF (50 ml) and stirred at room temperature for 48 h. The reaction mixture was poured into ice water (100 ml). The aqueous solution was acidified to pH 3 with concentrated HCl and the aqueous mixture extracted with Et_2O (3 × 50 ml). The combined organic layers were dried over anhydrous Na_2SO_4, filtered and evaporated in vacuo to leave the title compound **5** as a yellow oil (5.10 g, 95%). ^{1}H NMR ($CDCl_3$): δ 7.19–7.08 (m, 4H), 3.72–3.65 (m, 1H), 3.63 (s, 3H), 2.30 (s, 3H), 1.46 (d, J = 7.2 Hz, 3H). MS (EI): 179.1 $[M + H]^+$.

*6.1.4. Preparation of methyl 2-methyl-2-(4-methylphenyl) propanoate (**6**)*

A solution of methyl ester **5** (5.10 g, 28.6 mmol) in THF (30 ml) was added dropwise to a suspension of NaH (5.90 g, 0.148 mol) in n-hexane (30 ml) under argon atmosphere and stirred at room temperature for 30 min. MeI (14.6 g, 0.102 mol) was added to the reaction mixture and stirred at room temperature for 24 h. The reaction mixture was added to H_2O (50 ml) and extracted with Et_2O (3 × 50 ml). The organic layers were combined and dried over anhydrous Na_2SO_4, filtered and evaporated in vacuo to leave the title compound **6** as a yellow oil (2.72 g, 49%). ^{1}H NMR ($CDCl_3$): δ 7.23–7.09 (m, 4H), 3.63 (s, 3H), 2.31 (s, 3H), 1.56 (s, 6H). MS (EI): 193.1 $[M + H]^+$.

*6.1.5. Preparation of methyl 2-methyl-2-(4-bromomethylphenyl) propanoate (**7**)*

N-bromosuccinimide (3.00 g, 16.9 mmol) and benzoyl peroxide (catalytic amount) was added to a solution of intermediate **6** (2.72 g, 14.1 mmol) in CH_2Cl_2 (30 ml) and heated at reflux for 12 h. The reaction mixture was cooled to room temperature and filtered through a pad of silica gel. The filtrate was evaporated in vacuo to leave the title compound **7** as a yellow oil (2.32 g, 60%). ^{1}H NMR ($CDCl_3$): δ 7.33–7.23 (m, 4H), 4.46 (s, 2H), 3.63 (s, 3H), 1.55 (s, 6H). MS (EI): 271.0 $[M + H]^+$.

*6.1.6. Preparation of [1-[[4-(2-methoxy-1,1-dimethyl-2-oxo-ethyl) phenyl]methyl]-4-piperidinyl]methyl 3,4-dihydro-2H-[1,3]oxazino [3,2-a]indole-10-carboxylate (**8**)*

Bromomethyl ester **7** (0.40 g, 1.5 mmol) was added to a stirred suspension of piperidine amine **4** (0.47 g, 1.5 mmol) and K_2CO_3 (0.62 g, 4.5 mmol) in acetone (10 ml) and heated at reflux for 24 h. The mixture was cooled to room temperature, filtered and the filtrate evaporated in vacuo. The residue was redissolved in CH_2Cl_2 (20 ml) and washed with H_2O (3 × 5 ml). The organic layer was dried over Na_2SO_4, filtered and evaporated in vacuo. The residue was separated with flash chromatography (CH_2Cl_2/MeOH 9:1) to leave the title compound **8** as a white solid (0.34 g, 45%). ^{1}H NMR ($CDCl_3$): δ 7.97–7.92 (m, 1H), 7.25–7.16 (m, 5H), 7.14–7.10 (m, 2H), 4.51 (t, J = 5.2 Hz, 2H), 4.17 (d, J = 6.2 Hz, 2H), 4.08 (t, J = 6.2 Hz, 2H), 3.63 (s, 3H), 3.47 (s, 2H), 2.92–2.86 (m, 2H), 2.37–2.29 (m, 2H), 2.02–1.92 (m, 2H), 1.91–1.66 (m, 3H). 1,55 (s, 6H), 1.43–1.38 (m, 2H). MS (ES): 505.2 $[M + H]^+$.

*6.1.7. Preparation of 2-[4-[[4-(3,4-dihydro-2H-[1,3]oxazino[3,2-a] indole-10-carbonyloxymethyl)-1-piperidinyl]methyl]phenyl]-2-methylpropanoic acid (**9**)*

Methyl ester **8** (0.34 g, 0.67 mmol) was added to a mixture of 2 M aqueous NaOH (1 ml) and MeOH (4 ml) and stirred at reflux for 12 h. The mixture was cooled to room temperature and evaporated in vacuo. The residue was redissolved in H_2O (5 ml) and the solution acidified to pH 3 with 2 M aqueous HCl. The free carboxylic acid precipitate was filtered off and the residue recrystallized from acetone to leave the title compound **9** as a white solid (0.15 g, 46%); mp. 235–238 °C. ^{1}H NMR (DMSO-d_6): δ 12.10 (br s, 1 H), 7.81 (d, J = 5.9 Hz, 1H), 7.31–7.16 (m, 5H), 7.13–7.06 (m, 2H), 4.48 (t, J = 4.7 Hz, 2H), 4.10 (t, J = 6.0 Hz, 2H), 4.02 (d, J = 5.7 Hz, 2H), 3.38 (s, 2H), 2.85–2.80 (m, 2H), 2.26–2.21 (m, 2H), 2.01–1.91 (m, 2H), 1.72–1.67 (m, 3H), 1.44 (s, 6H), 1.32–1.22 (m, 2H). ^{13}C NMR (DMSO-d_6): δ 164.0, 154.8, 152.7, 132.1, 131.7, 127.7, 126.3, 125.5, 122.8, 121.2, 120.1, 109.7, 85.6, 80.0, 79.9, 67.4, 66.4, 59.6, 51.7, 35.2, 34.1, 31.8, 26.5, 21.1. HRMS (TOF MS ES+) for $C_{29}H_{34}N_2O_5$ $[M + H]^+$: calcd. 491.2468 found 491.2460.

*6.1.8. Preparation of [1-[[4-[1,1-dimethyl-2-[(5-methyl-2-oxo-1,3-dioxol-4-yl)methoxy]-2-oxo-ethyl]phenyl]methyl]-4-piperidinyl] methyl 3,4-dihydro-2H-[1,3]oxazino[3,2-a]indole-10-carboxylate hydrochloride (**10**)*

4-Chloromethyl-5-methyl-1,3-dioxol-2-one (78 mg, 0.53 mmol) was added to a suspension of carboxylic acid **9** (0.20 g, 0.40 mmol) and K_2CO_3 (0.16 g, 1.2 mmol) in dimethylacetamide (1.0 ml). The mixture was stirred at room temperature for 12 h, evaporated in vacuo and the residue separated by flash chromatography (CH_2Cl_2:MeOH 9:1) to leave the title compound **10** as a white solid (0.12 g, 50%). The corresponding hydrochloride salt was prepared by dissolving the title compound **10** in CH_2Cl_2 and adding ethereal HCl. After stirring for 1 h, the mixture was evaporated in vacuo and the residue recrystallized from acetone to leave the hydrochloride salt as a white crystalline solid; mp. 224–227 °C. ^{1}H NMR (DMSO-d_6): δ 10.30 (br s, 1 H), 7.80 (d, J = 6.7 Hz, 1H), 7.58–7.52 (m, 2H), 7.37–7.28 (m, 2H), 7.15–7.06 (m, 2H), 4.97 (s, 2H), 4.50 (t, J = 4.7 Hz, 2H), 4.22–4.21 (m, 2H), 4.11 (t, J = 5.9 Hz, 2H), 4.04 (d, J = 5.8 Hz, 2H), 3.31 (s, 2H), 2.94–2.91 (m, 2H), 2.26–2.22 (m, 2H), 2.11 (s, 3H), 1.93–1.89 (m, 3H), 1.63–1.55 (m, 2H), 1.51 (s, 6H). ^{13}C NMR (DMSO-d_6): δ 163.8, 154.6, 152.5, 149.9, 137.7, 134.4, 132.0, 131.7, 127.6, 126.2, 125.4, 122.8, 121.1, 120.1, 109.5, 85.4, 80.0, 79.7, 67.2, 66.2, 59.5, 51.6, 35.1, 34.0, 33.3, 31.6, 26.3, 21.0, 9.7. HRMS (TOF MS ES+) for $C_{34}H_{38}N_2O_8$ $[M + H]^+$: calcd. 603.2706 found 603.2699.

*6.1.9. Preparation of [1-[(4-tert-butylphenyl)methyl]-4-piperidinyl] methyl 3,4-dihydro-2H-[1,3]oxazino[3,2-a]indole-10-carboxylate hydrochloride (**11**)*

4-(*tert*-Butyl)-1-benzyl bromide (0.25 g, 1.0 mmol) was added to a stirred suspension of piperidine amine **4** (0.31 g, 1.0 mmol) and K_2CO_3 (0.41 g, 3.0 mmol) in acetone (10 ml) and heated to reflux for 24 h. The mixture was cooled to room temperature, filtered and the

filtrate evaporated in vacuo. The residue was redissolved in CH_2Cl_2 (20 ml) and washed with H_2O (3 × 5 ml). The organic layer was dried over Na_2SO_4, filtered and evaporated in vacuo. The residue was separated with flash chromatography (CH_2Cl_2/MeOH 9:1) to leave the title compound **11** as a white solid (0.27 g, 59%). The corresponding hydrochloride salt was prepared by dissolving the title compound **11** in CH_2Cl_2 and adding ethereal HCl. After stirring for 1 h, the mixture was evaporated in vacuo and the residue recrystallized from acetone to leave the hydrochloride salt as a white crystalline solid; mp. 216–220 °C. ^{1}H NMR (DMSO-d_6): δ 10.60 (s, 1H), 7.82-7.79 (m, 1H), 7.56–7.42 (m, 4H), 7.30 (d, J = 6.7 Hz, 1H), 7.17–7.08 (m, 2H), 4.50 (t, J = 4.7 Hz, 2H), 4.20–4.18 (m, 2H), 4.10 (t, J = 5.9 Hz, 2H), 4.03 (d, J = 5.8 Hz, 2H), 3.33–3.30 (m, 2H), 2.94–2.89 (m, 2H), 2.27–2.23 (m, 2H), 1.93–1.87 (m, 3H), 1.74–1.63 (m, 2H), 1.27 (s, 9H). ^{13}C NMR (DMSO-d_6): δ 154.8, 152.7, 132.1131.7, 127.7, 126.3, 125.5, 122.8, 121.2, 120.1, 109.7, 85.6, 67.4, 66.4, 59.6, 51.8, 35.2, 34.2, 31.9, 28.0, 26.5, 21.1, 21.0. HRMS (TOF MS ES+) for $C_{29}H_{36}N_2O_3$ $[M + H]^+$: calcd. 461.2803 found 461.2809.

6.2. Log $D_{Oct7.4}$ measurements

Compounds **9**, **10** and **11** (approximately 100 mg) were added to phosphate buffer pH 7.4 (50 ml) and the resulting solution filtered through a 0.43 μm filter. The phosphate buffer solutions (20 ml) were transferred to a separation funnel and added 1-octanol (20 ml), agitated for 24 h and set to reach equilibrium for 72 h at room temperature. The concentration of compounds **9**, **10** and **11** in samples of phosphate buffer and 1-octanol (n = 3) was quantified with LC-UV (Agilent Technologies 1100 series, equipped with degasser, autosampler, column oven and DAD detector). The logarithmic distribution coefficient was obtained using the following equation:

$$\log\ D_{\mathrm{Oct7,4}} = \log\ C_{\mathrm{Oct}}/C_{\mathrm{pH7.4}}$$

where C_{Oct} is the sum of ionized and unionized forms of compound **9**, **10** and **11** in 1-octanol and $C_{pH7.4}$ the corresponding concentrations in phosphate buffer pH 7.4.

6.3. Receptor binding and adenylyl cyclase assay

The experimental procedures to determine the competitive binding ([^{3}H]GR113808, 0.3 nM) and concentration-dependent inhibition of 5-HT-stimulated (1 μM) AC activity in membranes from HEK293 cells stably expressing the human 5-$HT_{4(b)}$ receptor have previously been described [12].

6.4. Effect on hERG tail current

The experimental work was carried out at Huntingdon Life Sciences (Cambridgeshire, England). Stock solutions of compound **9** and terfenadine (a known inhibitor of I_{kr}-current) were prepared in 100% DMSO. Test solutions were prepared in HEPES-buffered physiological external salt solutions (HB-PSS) with a final perfusion concentration of 0.1% DMSO.

Cells were cultured at 37 ± 1 °C in a humidified, gassed (set at 5% CO_2) incubator under standard conditions using Modified Eagle Medium (MEM + Glutamax) supplemented with 10% fetal bovine serum, 1% non-essential amino acids and 500 μg/ml geneticin. For patch-clamp experiments, cells were replated on sterile glass coverslips at low density to enable isolated cells to be selected for recording. Cells were incubated for 2–3 days prior to recording. Coverslips were transferred to a recording chamber mounted on the stage of an inverted microscope. The cells were continuously superfused with HB-PSS and only one cell per coverslip was used for experiments.

The whole-cell configuration was achieved first by forming a giga-ohm seal between the cell membrane and the patch pipette using gentle suction and then by rupturing the membrane patch under the electrode tip with a stronger suction pulse. The cell membrane potential was then clamped at −80 mV. Initial leak current was <100 pA and was subtracted using the amplifier and then continuously monitored at the holding potential (−80 mV) with an oscilloscope. Whole-cell patch-clamp recordings were performed using an Axopatch 200B amplifier (Molecular Devices, CA, USA) linked to a computer equipped with pCLAMP software (version 10.1). Data were filtered at 2 kHz and sampled using a Digidata analog-to-digital board.

The standard voltage protocol was run at 15 second intervals as follows: A step from −80 to +20 mV for 2 seconds activated hERG channels generating an outward current. A step from +20 to −50 mV for 2 seconds generated the tail current on which the effect of the test compound was determined. A step back to −80 mV returned the cell to the holding potential.

6.4.1. Treatment groups

Groups of cells were treated with vehicle solution, a single concentration of terfenadine and four concentrations of compound **9**. After a few minutes of equilibration, the voltage protocol was run a minimum of ten times to determine the tail current amplitude baseline before application of the vehicle, terfenadine or compound **9**. Ascending concentrations of compound **9** were applied sequentially and without washout between successive concentrations. Each concentration was applied until current inhibition had reached a steady state level. In order to construct the concentration-response curve for compound **9**, the process was repeated on several cells until at least 3 data points per concentration were obtained.

6.4.2. Data analysis

The data from the hERG current analysis were performed using the Clampfit module of pCLAMP software (version 10.2) and Microsoft Excel 2003. The peak hERG tail current amplitude was measured relative to the holding current at −80 mV and extracted into a spreadsheet where the tail current amplitude was calculated from an average of 5–10 voltage pulses. In the vehicle control group, the amplitude of the tail current over a period of approximately 22–23 min was recorded. For each cell, the tail current amplitude versus time was normalized against the first recorded current amplitude value. The data were then averaged for the three cells. For compound **9**, the peak amplitude of the tail current after exposure to each test concentration was measured and the percentage residual current calculated (% Baseline). To determine a concentration–response relationship for the effects of compound **9** on hERG tail current, the residual current calculated for each test concentration was individually corrected for the mean effect of vehicle and rundown observed using the corresponding (or closest minute) time-matched vehicle values as follows:

$$\%\ \mathrm{Baseline(vehicle\ \ corrected)} = \frac{\%\ \mathrm{Baseline(test\ \ substance)}}{\mathrm{mean}\ \ \%\ \mathrm{Baseline(time\ \ matched\ \ vehicle)}} \times 100$$

The corrected data were then averaged for each test concentration of compound **9**, plotted against nominal concentrations and the concentration–response curve was fitted using the following equation:

$$\%\ I_{\mathrm{Baseline}} = \mathrm{Bottom} + \frac{(\mathrm{Top} - \mathrm{Bottom})}{1 + 10^{n(ctp-x)}}$$

where x is the logarithm of the concentration of **9**, n is the Hill coefficient, Top and Bottom are respectively the top and bottom plateau and ctp is the logarithm of concentration of **9** at the curve turning point. The IC_{50} values for compound **9**, which is defined as the concentration at which hERG tail current is blocked by 50% after vehicle correction, were calculated from the above equation after the variables had been obtained from the fitting procedure.

6.5. Bioavailability and human liver microsomal stability studies

The bioavailability study was approved by the Animal Care and Use Committee of the State Provincial Office of Southern Finland. The experimental work for the bioavailability and microsomal stability studies were carried out at Novamass Ltd (Oulu, Finland) and Toxis Ltd Oy (Turku, Finland).

6.5.1. Animal model and sample preparations

Compounds **9** and **11** were dissolved in a solution of 10% ethanol in sterile water to a final concentration of 1.0 mg/ml. Compound **10** was dissolved in a 2% (w/v) aqueous solution of β-cyclodextrin to a final concentration of 1.0 mg/ml. Compounds **9**, **10** and **11** were dosed into male Sprague Dawley rats at 10 mg/kg for per-oral (p.o.) administration and for compound **9** at 1 mg/kg for i.v. administration. Blood samples were collected in Capiject® EDTA-K2 tubes from the lateral tail vein and by cardiac puncture (terminal samples) under isoflurane (4%) anesthesia at predefined time points (for compounds **9** and **11** three animals were used; p.o./i.v.: 5 min, 15 min, 30 min, 1 h, 2 h, 4 h, 8 h and 24 h, for compound **10** two animals were used; p.o.: 15 min, 30 min 1 h, 2 h, 4 h and 6 h and i.v.: 15 min, 30 min, 1 h, 2 h and 6 h). The exact time-points of dosing and sampling were recorded. The plasma was separated via centrifugation and frozen in −20 °C, shipped to the Novamass laboratory in dry ice and stored in −80 °C until analysis.

The plasma samples were thawed at room temperature, acidified with 1% formic acid (10% v/v) and protein precipitation performed with addition of acetonitrile (1:2 ratio of plasma to acetonitrile). The plasma samples were centrifuged for 10 min at 16 100 × g at room temperature (Eppendorf 5415D, Eppendorf AG, Hamburg, Germany) and the supernatants collected for analysis. The standard samples were similarly prepared, and blank plasma samples were spiked to analyte concentrations of 0.5, 1, 2, 5, 10, 20, 50, 100, 200, 500 (compounds **10** and **11**) and 1000 ng/ml (compound **9**). The determination coefficients (R^2) obtained were over 0.997 for all compounds. The plasma detection limit was less than 0.2 ng/ml for compounds **9** and **11** and 3 ng/ml for compound **10**. No peaks were detected after injection of blank rat plasma, suggesting good specificity of detection. The limit of quantitation was 0.5 ng/ml for compounds **9** and **11** and 5 ng/ml for compound **10**. The back-calculated accuracies were 85–125% for all compounds. The precisions were less than 11% for compounds **9** and **11** ($n = 3$) and the Snedecor-precision less than 7% ($n = 2$) for compound **10**.

6.5.2. Pharmacokinetic calculations

The pharmacokinetic parameters were calculated by WinNonlin Pro (Pharsight Corp., CA, USA) using standard non-compartment methods. Data from each animal was fitted individually and the resulting pharmacokinetic parameters were then averaged. The elimination phase half-life ($T_{1/2}$) was calculated by least-squares regression analysis of the terminal linear part of the concentration–time curve. The area under the plasma concentration–time curve was determined by use of the linear trapezoidal rule up to the last measurable concentration and thereafter by extrapolation of the terminal elimination phase to infinity. The maximum plasma concentration (C_{max}) and the time to C_{max} (T_{max}) were derived directly from the plasma concentration data. The tentative oral bioavailability (F) was calculated by dividing the dose normalized AUC after p.o. administration by the dose normalized AUC after i.v. administration, i.e.

$$F = [(\mathrm{AUC(p.o.)}/\mathrm{Dose(p.o.)})/(\mathrm{AUC(i.v)}/\mathrm{Dose(i.v.)})],$$

and reported as percentages (%). As compounds **10** and **11** are prodrugs of **9**, only the pharmacokinetic parameters for the free acid **9** were calculated. Since the number of animals for each time point for compound **10** was two, no statistical analysis of the results was carried out.

6.5.3. LC-MS for the bioavailability study

The quantitative LC-MS/MS data from the plasma samples were acquired with a Waters Acquity UPLC (Waters Corp., Milford, MA, USA) with an autosampler, a column oven and a vacuum degasser; together with a Waters Quattro Premier triple quadrupole mass spectrometer equipped with a Z-spray electrospray ion source. The analytical column used was a Waters BEH Shield RP18, (2.1 × 50 mm, 1.7 μm) together with an on-line filter. The eluents were 0.1% acetic acid (A, pH 3.2) and methanol (B). A linear gradient elution with profile 10%–10% – 90%–90% B in 0–1–2–2.5 min was employed, followed by column equilibration. The flow rate was 0.5 ml/min and the column oven temperature was 35 °C. Data was acquired using a multiple reaction monitoring (MRM) mode using positive ionization mode of electrospray. The first 1.0 min of the run was directed into waste by using a divert valve, to decrease the ion source contamination by early eluting matrix constituents. The mass spectrometer and UPLC system were operated under MassLynx 4.1 software.

6.5.4. Stability in human liver microsomal incubations

The pooled liver microsomes used contained 20 mg protein per ml and consisted of liver samples from 30 donors of both genders ((BD Biosciences Discovery Labware, Woburn, MA, USA). Compound **9** was incubated with liver microsomes in the presence of appropriate cofactors. The basic incubation mixture (250 μl) consisted of the following components: 0.5 mg of microsomal protein per ml, compound **9** dissolved in DMSO, 1 mM NADPH and 1 mM UDPGA. The final concentration of compound **9** was 2 μM. Two parallel incubates, one with cofactors and one without, were employed. Final amount of DMSO in the incubation was 1% (v/v). Each reaction mixture was preincubated for 2 min at + 37 °C in a shaking incubator block. Reaction was started by addition of NADPH and UDPGA. After incubation periods of 0, 10, 30 and 60 min, 50 μl samples were collected (without cofactors time points 0 and 60 min only) and the reaction terminated by adding an equal volume of ice-cold acetonitrile. Samples were subsequently cooled in an ice bath and the tubes were stored at −18 °C until analysis.

6.5.5. LC-MS for the stability study

The incubation samples were thawed at room temperature, shaken and centrifuged for 10 min at 16,100 × g and the supernatants pipetted to Maximum Recovery vials (Waters Corporation, Milford, MA, USA). The instrumental set up and analytical method was similar as for the bioavailability study. The flow was directed to MS via an Acquity photo-diode-array (PDA) detector. LC-TOF-MS data was recorded with a Waters LCT Premier XE time-of-flight mass spectrometer (Waters Corp., Milford, MA, USA) equipped with a LockSpray electrospray ionization source. A positive ionization mode of electrospray was used with a cone voltage of 60 V. The mass range of m/z 140–800 was acquired. Leucine enkephalin was used as the lock mass compound ($[M + H]^+$ m/z 556.2771) for accurate mass measurements. First 0.4 min of the run was directed into waste by using a divert valve, to decrease the ion source contamination by early eluting matrix constituents. No quantification was performed. The

disappearance of study substrate was determined by comparing the LC-MS peak area in the appropriate 0 min sample (without NADPH) to peak area of the corresponding metabolized sample, by using ion chromatograms created with ^{13}C-isotope peak. The metabolic profiles were determined by ESI-MS peak areas of molecular ion of a particular metabolite, assuming their responses to be directly comparable.

Conflict of interest

The compounds described in the present paper are described in WO2010112865 (Klaveness, J.; Brudeli, B.; Levy, F. O.; Moltzau, L. R.; Gulbrandsen, T.). This patent family is owned by Serodus AS where Andressen, Klaveness, Levy and Moltzau are shareholders.

Acknowledgments

This work was supported by The Research Council of Norway and Serodus AS. The authors wish to thank Trygve Gulbrandsen, Ph.D., COO of Serodus AS, for support, advice and discussions.

References

[1] J. Hannon, D. Hoyer, Behav. Brain Res. 195 (2008) 198–213.
[2] D.K. Arulmozhi, A. Veeranjaneyulu, S.L. Bodhankar, Vasc. Pharmacol. 43 (2005) 176–187.
[3] A.B. Kaumann, F.O. Levy, Pharmacol. Ther. 111 (2006) 674–706.
[4] E. Qvigstad, T. Brattelid, I. Sjaastad, K.W. Andressen, K.A. Krobert, J.A. Birkeland, O.M. Sejersted, A.J. Kaumann, T. Skomedal, J.-B. Osnes, F.O. Levy, Cardiovasc. Res. 65 (2005) 869–878.
[5] J.A.K. Birkeland, I. Sjaastad, T. Brattelid, E. Qvigstad, E.R. Moberg, K.A. Krobert, R. Bjørnerheim, T. Skomedal, O.M. Sejersted, J.-B. Osnes, F.O. Levy, Br. J. Pharmacol. 150 (2007) 143–152.
[6] J.K. Kjekshus, C. Torp-Pedersen, L. Gullestad, L. Køber, T. Edvardsen, I.C. Olsen, I. Sjaastad, E. Qvigstad, T. Skomedal, J.-B. Osnes, F.O. Levy, Eur. J. Heart Failure 11 (2009) 771–778.
[7] A. Sikander, S.V. Rana, K.K. Prasad, Clin. Chim. Acta 403 (2009) 47–55.
[8] F.D. Ponti, E. Poluzzi, A. Cavalli, M. Recanatini, N. Montanaro, Drug Saf. 25 (2002) 263–286.
[9] B. Zhu, Z.J. Jia, P. Zhang, T. Su, W. Huang, E. Goldman, D. Tumas, V. Kadambi, P. Eddy, U. Sinha, R.M. Scarborough, Y. Song, Bioorg. Med. Chem. Lett. 16 (2006) 5507–5512.
[10] F. Estelle, R. Simons, New Engl. J. Med. 351 (2004) 2203–2217.
[11] C. Chen, E. Hanson, J.W. Watson, J.S. Lee, Drug Metab. Dispos. 31 (2003) 312–318.
[12] B. Brudeli, L.R. Moltzau, K.W. Andressen, K.A. Krobert, J. Klaveness, F.O. Levy, Bioorg. Med. Chem. 18 (2010) 8600–8613.
[13] M.A. Alisi, N. Cazzolla, R. Costi, R. Di Santo, G. Furlotti, A. Guglielmotti, L. Polenzani, PCT Int. Appl. (July 29, 2008)WO2010/012611A1.
[14] M. Fedouloff, F. Hossner, M. Voyle, J. Ranson, J. Powles, G. Riley, G. Sanger, Bioorg. Med. Chem. 9 (2001) 2119–2128.
[15] L.M. Gaster, F.D. King, Med. Res. Rev. 17 (1997) 163–214.
[16] M.L. López-Rodríguez, B. Benhamú, A. Viso, M.J. Morcillo, M. Murcia, L. Orensanz, M.J. Alfaro, M.I. Martın, Bioorg. Med. Chem. 7 (1999) 2271–2281.
[17] H.J. Witchel, Cardiovasc. Ther. 29 (2011) 251–259.
[18] L. Kiss, P.B. Bennett, V.N. Uebele, K.S. Koblan, S.A. Kane, B. Neagle, K. Schroeder, Assay Drug Dev. Technol. 1 (2003) 127–135.
[19] R. Waterhouse, Mol. Imaging Biol. 5 (2003) 376–389.
[20] S.D. Krämer, N.J. Abbott, D.J.A. Begley, Biological models to study blood-brain barrier permeation, in: B. Testa, H. Waterbeemd, G. Folkers, R.H. Guy (Eds.), Pharmacokinetic Optimization in Drug Research: Biological, Physiochemical and Computational Strategies, Wiley-VHCA, Zürich, 2001, pp. 127–153.
[21] X. Liu, B. Testa, A. Fahr, Pharm. Res. 28 (2011) 962–977.
[22] V.A. Levin, J. Med. Chem. 23 (1980) 682–684.
[23] W.M. Pardridge, D. Triguero, J. Yang, P.A. Cancilla, J. Pharmacol. Exp. Ther. 253 (1990) 884–891.
[24] H. Ansanay, A. Dumuis, M. Sebben, J. Bockaert, L. Fagni, Proc. Natl. Acad. Sci. U. S. A. 92 (1995) 6635–6639.
[25] G.E. Torres, Y. Chaput, R. Andrade, Mol. Pharmacol. 47 (1995) 191–197.
[26] H. Mei, W. Korfmacher, R. Morrison, AAPS J. 8 (2006) E493–E450.
[27] B. Davies, T. Morris, Pharm. Res. 10 (1993) 1093–1095.
[28] M. Langlois, R. Fischmeister, J. Med. Chem. 46 (2003) 319–344.
[29] P. Ettmayer, G.L. Amidon, B. Clement, B. Testa, J. Med. Chem. 47 (2004) 2393–2404.
[30] L.J. Scott, P.L. McCormack, Drugs 68 (2008) 1239–1272.
[31] D.E. Mire, T.N. Silfani, M.K. Pugsley, J. Cardiovasc. Pharmacol. 46 (2005) 583–593.
[32] P. Laeis, K. Puchler, W. Kirch, J. Hypertens. (Suppl. 19) (2001) S21–S32.